Superfluid Density in a Highly Underdoped $YBa_2Cu_3O_{6+y}$ Superconductor

D. M. Broun,[1] W. A. Huttema,[1] P. J. Turner,[1] S. Özcan,[2] B. Morgan,[2] Ruixing Liang,[3] W. N. Hardy,[3] and D. A. Bonn[3]

[1]*Department of Physics, Simon Fraser University, Burnaby, British Columbia, Canada V5A 1S6*

[2]*Cavendish Laboratory, Madingley Road, Cambridge CB3 0HE, United Kingdom*

[3]*Department of Physics and Astronomy, University of British Columbia, Vancouver, British Columbia, Canada V6T 1Z1*

(Received 28 July 2007; published 7 December 2007)

The superfluid density $\rho_s(T) \equiv 1/\lambda^2(T)$ has been measured at 2.64 GHz in highly underdoped $YBa_2Cu_3O_{6+y}$, at 37 dopings with T_c between 3 and 17 K. Within limits set by the transition width $\Delta T_c \approx 0.4$ K, $\rho_s(T)$ shows no evidence of critical fluctuations as $T \to T_c$, with a mean-field-like transition and no indication of vortex unbinding. Instead, we propose that ρ_s displays the behavior expected for a quantum phase transition in the $(3+1)$-dimensional XY universality class, with $\rho_{s0} \propto (p - p_c)$, $T_c \propto (p - p_c)^{1/2}$, and $\rho_s(T) \propto (T_c - T)^1$ as $T \to T_c$.

DOI: 10.1103/PhysRevLett.99.237003 PACS numbers: 74.72.Bk, 74.25.Bt, 74.25.Ha, 74.25.Nf

Current research on high temperature superconductivity focuses on the underdoped cuprates, in a region of the phase diagram where d-wave superconductivity gives way to antiferromagnetism [1]. One proposal for this regime is that at temperatures up to about 100 K above T_c, superconductivity persists locally, with long-range phase coherence suppressed by fluctuations in the phase of the superconducting order parameter [2–8]. Early results showing a linear relation between T_c and the superfluid density $\rho_s(T = 0)$ [9] provided the original motivation for this point of view, suggesting that T_c is low in underdoped materials because the phase stiffness is low. Further support for this idea has come from measurements showing a finite phase stiffness above T_c at terahertz frequencies [10], and from experiments that appear to detect the phase-slip voltage of thermally diffusing vortices in the normal state [11]. If the physics of the underdoped cuprates is indeed that of a fluctuating d-wave superconductor, there should be a regime where quantum fluctuations come into play as T_c falls to zero with decreasing doping. Here we test this idea with a detailed study of the doping dependence of the superfluid density in the vicinity of the critical doping for superconductivity.

High homogeneity of T_c is particularly difficult to achieve in the underdoped cuprates, where the control parameter is chemical doping and the materials are well away from plateaus or turning points in $T_c(y)$. The $YBa_2Cu_3O_{6+y}$ system has two advantages in this doping range: with careful work, there can be sufficient control of doping homogeneity to produce samples with sharp superconducting transitions [12,13]; and the process of CuO-chain ordering can be harnessed to provide continuous tunability of the carrier density in a *single* sample, with *no* change in cation disorder [14]. This is possible because the loosely held chain oxygen atoms in these high quality samples remain mobile at room temperature and gradual ordering into CuO-chain structures slowly pulls electrons from the CuO_2 planes, smoothly increasing hole doping over time [15,16]. For this experiment, single crystals of $YBa_2Cu_3O_{6+y}$ were grown in barium zirconate crucibles and have high purity and low defect levels, with cation disorder at the 10^{-4} level [17]. A crystal 0.3 mm thick was cut and polished with Al_2O_3 abrasive into an ellipsoid of revolution about the sample c axis, 0.35 mm in diameter. The oxygen content of the ellipsoid was adjusted to $O_{6.333}$ by annealing at 914 °C in flowing oxygen, followed by a homogenization anneal in a sealed quartz ampoule at 570 °C and a quench to 0 °C. At this point the sample was nonsuperconducting. After allowing chain oxygen order to develop at room temperature for three weeks, T_c was 3 K. The sample was then further annealed at room temperature for six weeks under hydrostatic pressure of $\sim$30 kbar, raising T_c to 17 K. The sample was cooled to -5 °C, removed from the pressure cell, and then stored at -10 °C to prevent the oxygen order from relaxing. All further manipulation of the ellipsoid was carried out in a refrigerated glove box at temperatures less than -5 °C. In between measurements of surface impedance, periods of controlled *in situ* annealing at room temperature and ambient pressure were used to generate a sequence of 36 dopings as T_c relaxed back to 3 K. We emphasize that no oxygen entered or left the sample during these annealing steps. Subsequent reannealing under hydrostatic pressure, for a further six weeks, returned T_c to the starting value of 17 K, where the sample was remeasured to demonstrate the reversibility of the technique.

Measurements of the ab-plane surface impedance $Z_s = R_s + iX_s$ were carried out at 2.64 GHz by cavity perturbation, using a sapphire hot finger to position the sample at the H-field antinode of the $TE_{01\delta}$ mode of a rutile dielectric resonator [18]. All data sets reported here were taken with the c axis of the ellipsoid oriented along the microwave magnetic field H_{rf} to induce ab-plane screening currents. The surface impedance of the sample has been obtained from the measured cavity response using the cavity perturbation formula $\Delta f_B(T) - 2i\Delta f_0(T) = \Gamma(R_s + i\Delta X_s)$, where $\Delta f_B(T)$ is the change in bandwidth of the $TE_{01\delta}$ mode upon inserting the sample into the cavity, and $\Delta f_0(T)$ is the shift in resonant frequency upon warming the sample from base temperature to T. Γ

is a scale factor that applies to the data set as a whole and is empirically determined using a Pb–Sn replica sample to an accuracy of 2.5%. The absolute surface reactance is set in the usual way by matching R_s and X_s in the normal state, where we expect the imaginary part of the microwave conductivity to be very small. This is illustrated in Fig. 1, which shows the surface impedance $Z_s = R_s + iX_s$ of the ellipsoid at two of the dopings. The rounded shoulders in $Z_s(T)$ are the result of fluctuations. This is seen more clearly in the microwave conductivity $\sigma = \sigma_1 - i\sigma_2$, which is obtained using the local-limit expression $\sigma = i\omega\mu_0/Z_s^2$. The inset of Fig. 1 shows $\sigma_1(T)$ at one of the dopings, revealing a narrow fluctuation peak at T_c. In a homogeneous system, $\sigma_1(T)$ is expected to have a sharp cusp at T_c [19]. Rounding of the fluctuation peak, arising from the macroscopic dopant inhomogeneity present in all real samples, is used to define ΔT_c.

The superfluid density is given by $\rho_s \equiv 1/\lambda^2 = \omega\mu_0\sigma_2$. Figure 2 shows $\rho_s(T)$ at 20 of the 37 dopings. The most striking feature of the data is the wide range of linear temperature dependence, extending from close to T_c down to $T \approx 4$ K. Below 4 K $\rho_s(T)$ crosses over to an accurately quadratic temperature dependence. Such behavior is well established in $YBa_2Cu_3O_{6+y}$ at higher dopings and is consistent with d-wave superconductivity in the presence of a small density of pair-breaking defects [20,21]. One unusual feature of the data is the nature of the thermal transitions, which, within limits set by ΔT_c, appear mean-field-like. At optimal doping $YBa_2Cu_3O_{6+y}$ is the most three-dimensional cuprate, with $\lambda_c^2(T \to 0)/\lambda_{ab}^2(T \to 0) \approx 50$ [22]. Its critical behavior has been firmly established to be in the 3D-XY universality class [23–25]. In the doping range explored in this Letter, $YBa_2Cu_3O_{6+y}$ is highly anisotropic, with $\lambda_c^2(T \to 0)/\lambda_{ab}^2(T \to 0) \approx 10\,000$ [14]. In these circumstances, one would anticipate fluctuations in adjacent layers to be uncorrelated, and a Kosterlitz-Thouless-Berezinsky (KTB) vortex-unbinding transition [6,26] should occur when the 2D phase stiffness in a layer of thickness d, $\rho_s^{2D}(T) \equiv \hbar^2 d/4k_B e^2 \mu_0 \lambda^2(T)$, falls to $(2/\pi)T$. This defines minimum superfluid densities for isolated planes and CuO_2 bilayers, shown in Fig. 2 by the dashed and solid lines, respectively. $\rho_s(T)$ instead passes smoothly through these lines, with no indication of vortex unbinding. Surprisingly, this implies that fluctuations remain correlated over many unit cells in the c direction. Recent work on $YBa_2Cu_3O_{6+y}$ thin films supports this, showing that the KTB transition does occur but that the effective thickness for fluctuations is the film thickness [27]. At the highest dopings in our experiment, $\rho_s(T)$ develops slight downward curvature

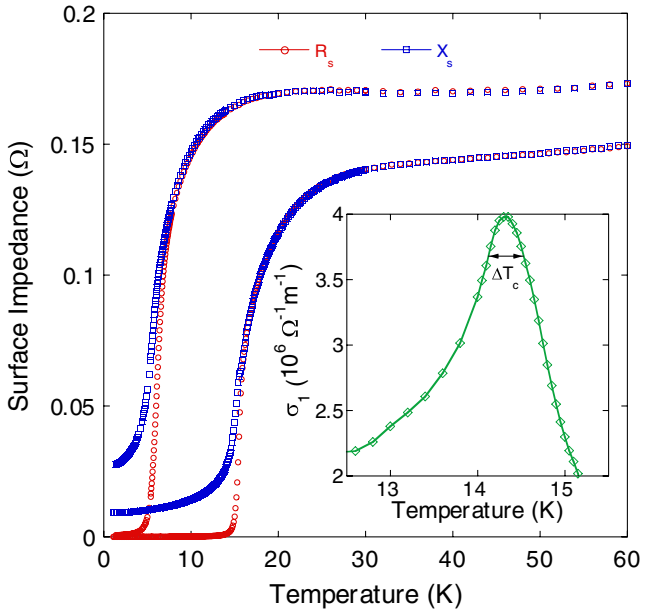

FIG. 1 (color online). ab-plane surface impedance at 2.64 GHz for the $YBa_2Cu_3O_{6+y}$ ellipsoid, at two dopings. $R_s(T)$ is measured directly in the experiment. Absolute reactance is obtained by offsetting $\Delta X_s(T)$ so that R_s and X_s match in the normal state. Inset: a fluctuation peak in $\sigma_1(T)$ at one doping. ΔT_c is set to the difference between inflection points in $\sigma_1(T)$ on opposite sides of the transition.

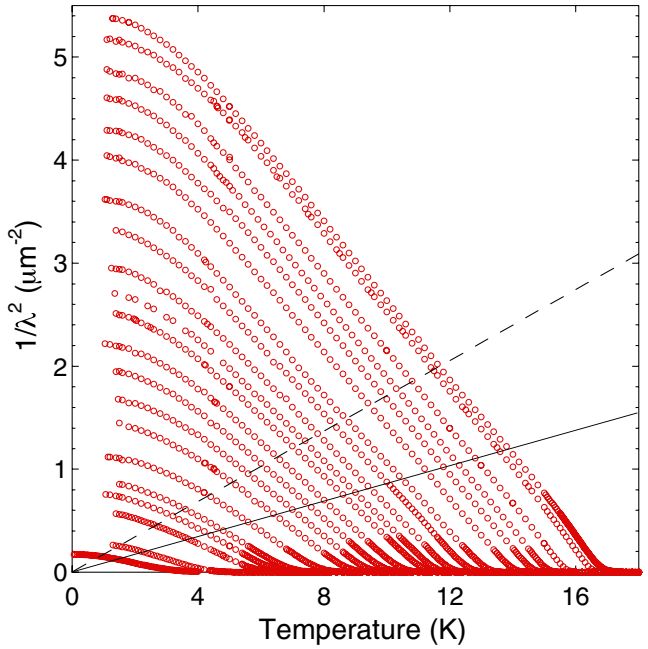

FIG. 2 (color online). ab-plane superfluid density $\rho_s(T) = 1/\lambda^2(T)$ shown at 20 of the 37 dopings measured in this study. Measurements were made starting in the most ordered state ($T_c \approx 17$ K) followed by controlled oxygen annealing in small steps down to $T_c \approx 3$ K. At the end of the experiment the sample was reordered and measured again to verify reproducibility. Lines mark where the vortex-unbinding transition should occur for a 2D superconductor. The dashed line corresponds to $\rho_s^{2D} \equiv \hbar^2 d/4k_B e^2 \mu_0 \lambda^2 = (2/\pi)T$ in each CuO_2 plane. The solid line shows $\rho_s^{2D} = (2/\pi)T$ in each CuO_2 bilayer. $\rho_s(T)$ instead passes smoothly through this region. While mean-field-like over most of the doping range, $\rho_s(T)$ develops downwards curvature near T_c at the highest dopings, a possible indication of the onset of the 3D-XY critical fluctuations.

near T_c, possibly indicating the emergence of 3D-XY criticality.

Previous studies of superfluid density in the underdoped cuprates have focused on the strong correlation between T_c and $\rho_{s0} \equiv 1/\lambda^2(T \to 0)$ [9,28]. Our new data, taken on a single, high purity crystal, explore the highly underdoped region in considerably more detail. The strong correlation between T_c and ρ_{s0} remains, but ρ_{s0} is up to an order of magnitude larger than in the earlier work on thin films [28]. As in the thin film study, ρ_{s0} falls continuously to zero on underdoping and varies approximately quadratically with T_c at low doping. Recent experiments on the CuO_2 plane doping state in $YBa_2Cu_3O_{6+y}$ have established a mapping between $T_c(y)$ and p, the hole concentration per planar Cu [13]. In Fig. 3, a linear fit to the $T_c(p)$ data from Ref. [13] has been used to determine p and plot $\rho_{s0}(p)$. At higher doping ρ_{s0} has a linear doping dependence. This behavior appears to be very robust: an extrapolation of the linear fit in Fig. 3 passes within 5% of the ab-averaged superfluid density of Ortho-II $YBa_2Cu_3O_{6+y}$ [22]. To the extent that the linear extrapolation of $T_c(p)$ holds, $\rho_{s0}(p)$ varies approximately quadratically close to the onset of superconductivity. However, as we will discuss below, this quadratic behavior is difficult to understand theoretically. Later on we will present an alternative proposal in which it is ρ_{s0}, not T_c, whose linear doping dependence extends to the edge of the superconducting phase.

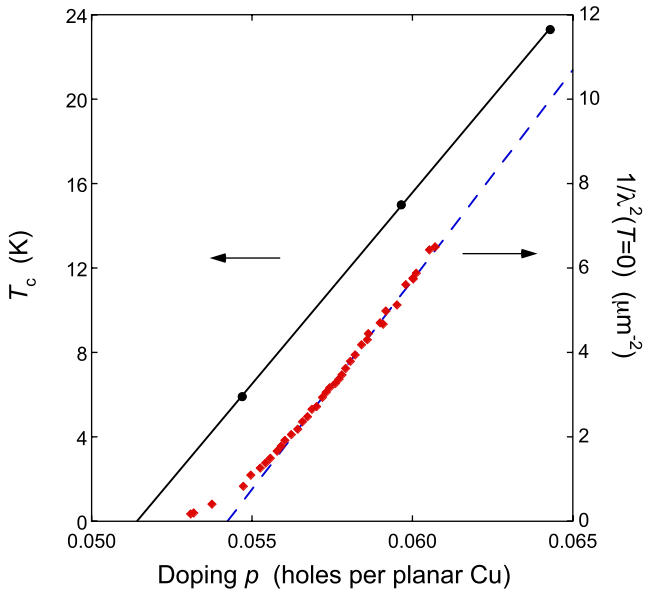

FIG. 3 (color online). Our $\rho_{s0}(p)$ data (solid diamonds, right-hand scale) and $T_c(p)$ data from Ref. [13] (solid circles, left-hand scale). $\rho_{s0} \equiv 1/\lambda^2(T \to 0)$ is obtained by linear extrapolation to $T = 0$. Hole doping for the superfluid density data is determined from our values of T_c, using a linear fit and extrapolation of the $T_c(p)$ data from Ref. [13] (solid line). To the extent that this extrapolation is valid, $\rho_{s0}(p) \sim (p - p_c)^2$ at the onset of superconductivity, before crossing over to a linear doping dependence. The dashed line is a linear fit to $\rho_{s0}(p)$ at higher doping.

The very low superfluid density, its continuous variation with doping, and the importance of 3D-XY fluctuations near optimal doping [23–25] together suggest that close to the critical doping, p_c, the transition out of the superconducting state may be controlled by fluctuations near a quantum critical point. In the scaling theory of a quantum phase transition, physical properties are related to a single, divergent correlation length, $\xi \propto |x|^{-\nu}$, where $x = (p - p_c)$. Scaling analysis of the XY model predicts $T_c \propto \xi^{-z} \propto |x|^{\nu z}$ and $\rho_{s0} \propto \xi^{-(d-2+z)} \propto |x|^{\nu(d-2+z)}$, where z is the dynamical critical exponent [6,29,30]. Together, these relations imply $T_c \propto \rho_{s0}^{z/(d-2+z)}$, independent of ν. In $d = 2$ this requires $T_c \propto \rho_{s0}$, whereas our experiments show $T_c \sim \rho_{s0}^{1/2}$. In $d = 3$, $T_c \propto \rho_{s0}^{z/(1+z)}$ and is consistent with our observations if $z = 1$, the so-called (3 + 1)D-XY universality class [8]. $D = 4$ is the upper critical dimension of the XY model, so mean-field critical behavior ($\nu = \frac{1}{2}$) should follow. However, this choice of ν is not compatible with the doping dependences of T_c and ρ_{s0} shown in Fig. 3: scaling arguments predict $T_c \propto x^{1/2}$ and $\rho_{s0} \propto x$, whereas the analysis shown in Fig. 3 has $T_c \propto x$ and therefore $\rho_{s0} \propto x^2$. This difficulty may well stem from our determination of doping in Fig. 3, which is based on a linear fit and extrapolation of the $T_c(p)$ data from Ref. [13]. The sparseness of the $T_c(p)$ data, along with the lack of an anchor point as $T_c \to 0$, allows a different interpretation in the low doping regime. In Fig. 3, all data with $T_c \geq 8$ K follow an accu-

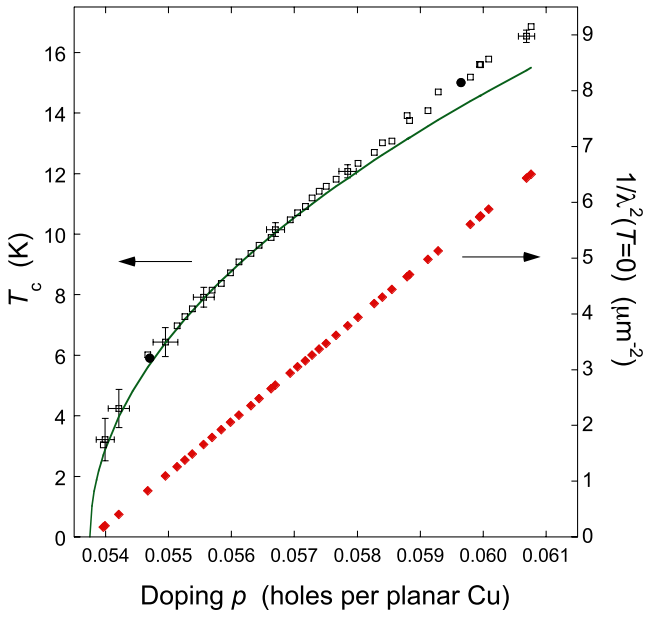

FIG. 4 (color online). The results of assuming a linear mapping between doping and ρ_{s0} (solid diamonds). T_c (open squares) varies as $(p - p_c)^{1/2}$ as $p \to p_c$, with the solid line a square-root $T_c(p)$ curve for comparison. $T_c(p)$ data from Ref. [13] (solid circles) are sparse in this range. Vertical bars on the T_c data show transition widths estimated from rounding of $\sigma_1(T)$ fluctuation peaks. The corresponding doping spreads (horizontal bars) show little variation with doping.

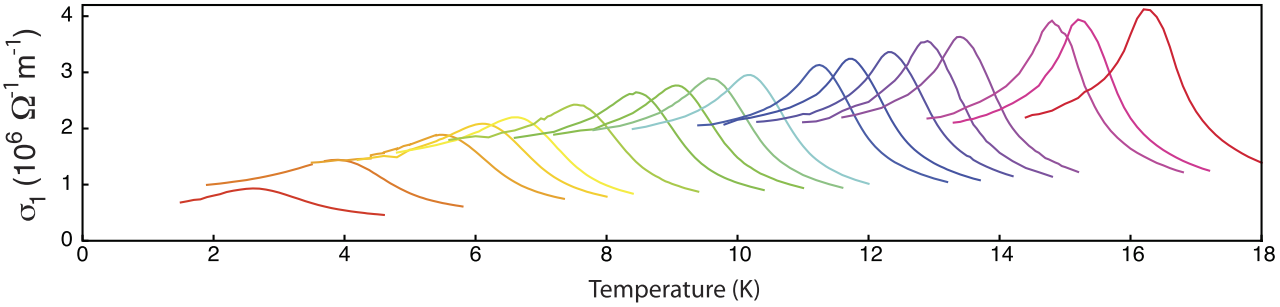

FIG. 5 (color online). Fluctuation peaks in $\sigma_1(T)$ at 2.64 GHz as doping is varied. Peak width is approximately constant in the higher doping range and then broadens considerably below $T_c \approx 8$ K, consistent with a steepening of $T_c(p)$ in that range.

rately linear doping dependence of ρ_{s0}, which seems to extrapolate well to much higher dopings. The robustness of this form leads us to put forward the following suggestion as a means of understanding the data. We propose that $\rho_{s0}(p)$ is, in actual fact, proportional to $(p - p_c)$ in the low doping range and use this linear mapping to determine $T_c(p)$. The results of this analysis are shown in Fig. 4. The mapping leaves $T_c(p)$ consistent with the data of Ref. [13]; the effect is simply to refine the $T_c(p)$ curve in the vicinity of the critical doping. $T_c(p)$ now grows initially as $(p - p_c)^{1/2}$, in accord with scaling arguments, before crossing over to a linear doping dependence at higher dopings. Over a substantial doping range this yields the well-known result that T_c scales approximately with ρ_{s0} [9]. In addition, our proposed interpretation gives a plausible explanation of another aspect of the data. At the lowest dopings, the fluctuation peaks in $\sigma_1(T)$ broaden considerably, as shown in Figs. 4 and 5. In the presence of small, macroscopic variations in oxygen concentration, such broadening would be a natural consequence of a steepening of $T_c(p)$ on the approach to p_c. Future experiments, including those of the sort carried out in Ref. [13], will be needed to confirm our conjecture. However, the proposed scenario has several compelling features, not least of which is a substantial simplification of our theoretical picture of the transition from nonsuperconductor to superconductor in the underdoped cuprates.

In summary, at the critical doping for superconductivity ρ_{s0} becomes nonzero and appears to grow linearly with doping, at a rate that remains constant up to much higher doping. Fluctuations in the low doped range are three dimensional, with no indication of the physics of 2D vortex unbinding, and with critical exponents characteristic of $(3 + 1)$D-XY universality. Quantum fluctuations appear to control T_c in the critical region, with $T_c \propto (p - p_c)^{1/2}$, but become less effective at depleting ρ_s away from p_c, allowing $T_c(p)$ to cross over to a linear doping dependence.

We acknowledge useful discussions with A. J. Berlinsky, M. J. Case, S. Chakravarty, J. Cooper, J. C. Davis, J. S. Dodge, M. Franz, I. F. Herbut, S. Kivelson, J. E. Sonier, and Z. Tešanović. This work was funded by the National Science and Engineering Research Council of Canada and the Canadian Institute for Advanced Research.

[1] J. Orenstein and A. J. Millis, Science **288**, 468 (2000).
[2] V. J. Emery and S. A. Kivelson, Nature (London) **374**, 434 (1995).
[3] M. Franz and Z. Tešanović, Phys. Rev. Lett. **87**, 257003 (2001); M. Franz, Z. Tešanović, and O. Vafek, Phys. Rev. B **66**, 054535 (2002).
[4] I. F. Herbut, Phys. Rev. Lett. **88**, 047006 (2002).
[5] I. F. Herbut, Phys. Rev. B **66**, 094504 (2002).
[6] I. F. Herbut and M. J. Case, Phys. Rev. B **70**, 094516 (2004).
[7] I. F. Herbut, Phys. Rev. Lett. **94**, 237001 (2005).
[8] M. Franz and A. P. Iyengar, Phys. Rev. Lett. **96**, 047007 (2006).
[9] Y. J. Uemura *et al.*, Phys. Rev. Lett. **62**, 2317 (1989).
[10] J. Corson *et al.*, Nature (London) **398**, 221 (1999).
[11] Y. Wang *et al.*, Science **299**, 86 (2003).
[12] R. Liang *et al.*, Physica (Amsterdam) **383C**, 1 (2002).
[13] R. Liang, D. A. Bonn, and W. N. Hardy, Phys. Rev. B **73**, 180505 (2006).
[14] A. Hosseini *et al.*, Phys. Rev. Lett. **93**, 107003 (2004).
[15] J. Zaanen *et al.*, Phys. Rev. Lett. **60**, 2685 (1988).
[16] B. W. Veal *et al.*, Phys. Rev. B **42**, 6305 (1990).
[17] R. Liang, D. A. Bonn, and W. N. Hardy, Physica (Amsterdam) **304C**, 105 (1998).
[18] W. A. Huttema *et al.*, Rev. Sci. Instrum. **77**, 023901 (2006).
[19] D. S. Fisher, M. P. A. Fisher, and D. A. Huse, Phys. Rev. B **43**, 130 (1991).
[20] D. A. Bonn *et al.*, Phys. Rev. B **50**, 4051 (1994).
[21] P. J. Hirschfeld and N. Goldenfeld, Phys. Rev. B **48**, R4219 (1993); P. J. Hirschfeld, W. O. Putikka, and D. J. Scalapino, Phys. Rev. B **50**, 10250 (1994).
[22] T. Pereg-Barnea *et al.*, Phys. Rev. B **69**, 184513 (2004).
[23] S. Kamal *et al.*, Phys. Rev. Lett. **73**, 1845 (1994).
[24] A. Junod *et al.*, Physica (Amsterdam) **280B**, 214 (2000).
[25] C. Meingast *et al.*, Phys. Rev. Lett. **86**, 1606 (2001).
[26] L. B. Ioffe and A. J. Millis, J. Phys. Chem. Solids **63**, 2259 (2002).
[27] Y. Zuev *et al.*, arXiv:cond-mat/0407113; I. Hetel, T. R. Lemberger, and M. Randeria, Nature Phys. **3**, 700 (2007).
[28] Y. Zuev, M. S. Kim, and T. R. Lemberger, Phys. Rev. Lett. **95**, 137002 (2005).
[29] A. Kopp and S. Chakravarty, Nature Phys. **1**, 53 (2005).
[30] S. Sachdev, *Quantum Phase Transitions* (Cambridge University Press, Cambridge, England, 1999).